Mon. Not. R. Astron. Soc. **000**, 000–000 (0000) Printed 5 September 2014 (MN LATEX style file v2.2)

Luminosity function and jet structure of Gamma Ray Bursts

A. Pescalli[1,2⋆], G. Ghirlanda[2], O. S. Salafia[1,2] G. Ghisellini[2], F. Nappo[3,2], R. Salvaterra[4]

[1]*Dipartimento di Fisica G. Occhialini, Universita? di Milano Bicocca, Piazza della Scienza 3, I-20126 Milano, Italy*
[2]*INAF – Osservatorio Astronomico di Brera, via E. Bianchi 46, I-23807 Merate, Italy*
[3]*Universita' degli Studi dellInsubria, via Valleggio 11, I-22100 Como, Italy*
[4]*INAF – IASF Milano, via E. Bassini 15, I-20133 Milano, Italy*

arXiv:1409.1213v1 [astro-ph.HE] 3 Sep 2014

ABSTRACT

The structure of Gamma Ray Burst (GRB) jets impacts on their prompt and afterglow emission properties. The jet of GRBs could be *uniform*, with constant energy per unit solid angle within the jet aperture, or it could instead be *structured*, namely with energy and velocity that depend on the angular distance from the axis of the jet. We try to get some insight about the still unknown structure of GRBs by studying their luminosity function. We show that low (10^{46-48} erg s^{-1}) and high (i.e. with $L \geqslant 10^{50}$ erg s^{-1}) luminosity GRBs can be described by a unique luminosity function, which is also consistent with current lower limits in the intermediate luminosity range (10^{48-50} erg s^{-1}). We derive analytical expressions for the luminosity function of GRBs in uniform and structured jet models and compare them with the data. Uniform jets can reproduce the entire luminosity function with reasonable values of the free parameters. A structured jet can also fit adequately the current data, provided that the energy within the jet is relatively strongly structured, i.e. $E \propto \theta^{-k}$ with $k \geqslant 4$. The classical $E \propto \theta^{-2}$ structured jet model is excluded by the current data.

Key words: Gamma-ray burst: general; radiation mechanisms: non-thermal; relativistic processes

1 INTRODUCTION

Jets are a common feature of high energy astrophysical sources powered by accretion onto compact objects. GRB jets are thought to be the most extreme in terms of typical power (10^{50-54} erg s^{-1}) and of Lorentz factor ($\Gamma \sim 10^2 - 10^3$). Long GRBs are thought to follow the gravitational collapse of massive stars which form a rotating black hole with a bipolar jet along its rotational axis. The large isotropic equivalent energy $E_{\rm iso}$ of the prompt emission can exceed a solar mass rest energy, unless the radiation is collimated (Tan, Matzner & McKee 2001). The observed steepening of the afterglow flux light curve a few days after the burst is interpreted as the direct evidence of the presence of collimation.

It has been typically assumed that GRBs have a *Uniform Jet* (UJ): the energy and ejecta velocity are constant, within the jet aperture, and zero outside the jet opening angle (i.e. sharp–edged jet). During the afterglow phase, when the emission is produced by the deceleration of the relativistic jet by the interstellar medium, a steepening of the observed afterglow flux is predicted when $\Gamma \sim 1/\theta_{\rm j}$ (Rhoads 1997; Sari, Piran & Halpern 1999). The measure of the time of this break ($t_{\rm break}$) has been used to infer the jet opening angle $\theta_{\rm j}$ which results distributed in the 1°–10° range. Intriguingly, the true energetic of GRBs (i.e. accounting for their collimation) clusters around a typical value $E_\gamma = E_{\gamma,\rm iso}(1-\cos\theta_{\rm j}) \approx 10^{51}$ erg with a dispersion of less than a decade (Frail et al. 2001), correlating with the peak energy of the prompt emission spectrum $E_{\rm peak}$ (Ghirlanda et al. 2004; Nava et al. 2006). Such typical value for the true energy of GRBs is also directly probed by late time radio observations (Frail, Waxman & Kulkarni 2000; Frail et al. 2005; Shivvers & Berger 2011).

For small jet angles, the collimation corrected $E_\gamma \propto \theta_{\rm j}^2 E_{\gamma,\rm iso}$. The small dispersion of E_γ led to the idea that the jet is not uniform, but *structured*, where θ is the angular distance from the jet axis, and coincides with the viewing angle $\theta_{\rm v}$. This scenario assumes that what we believed to be the jet angle $\theta_{\rm j}$ is actually the viewing angle $\theta_{\rm v}$. This can lead to a unification scheme in which all bursts are basically equal, but appear different only because they are seen under different angles. If the dependence of the burst energetics on θ is $E_{\gamma,\rm iso} \propto \theta^{-2}$, one recovers the finding of Frail et al. (2001) of the clustering of E_γ. These GRBs with a universal structured jet (SJ) were first proposed by Lipunov, Postnov & Prokhorov (2001) and then studied by Rossi, Lazzati & Rees (2002) and Zhang & Meszaros (2002). Some structure to the jet power and velocity could be imprinted, within the collapsar model, by the interaction of the jet with the star (e.g. Zhang, Woosley & Mac Fadyen 2003; Zhang, Woosley & Heger 2004; Lazzati & Begelman 2005; Morsony, Lazzati & Begelman 2010; Levinson & Eichler 2003; Lyu-

⋆ E–mail:a.pescalli@campus.unimib.it

© 0000 RAS

tikov & Blandford 2002) or instead the SJ could have an "external" origin (Ghisellini et al. 2007).

Direct tests of the SJ model with available data, e.g. the search for a possible anti correlation between $E_{\gamma,\rm iso}$ and $\theta_{\rm v}$ (Perna, Sari & Frail 2003; Lloyd–Ronning, Dai & Zhang 2004) or the statistical studies of the flux cumulative distribution of large GRB samples in the SJ model, did not provide definite evidence for this model (Nakar, Granot & Guetta 2004; Cui, Liang & Lu 2005). However, the presence of a structured jet is invoked to interpret some GRBs with a double jet break in their afterglow light curves (e.g. GRB 991216 – Frail et al. 2000; GRB 030329 – Berger et al. 2003, Sheth et al. 2003; GRB 021004 - Starling et al. 2005). In these cases, a "discrete" SJ model composed by a narrow jet surrounded by a wider cone was proposed (Peng, Koenigl & Granot 2005), possibly due to the interaction of the jet with the star cocoon (Ramirez–Ruiz, Celotti & Rees 2002; Vlahkis, Peng & Koenigl 2003; Lazzati & Begelman 2005).

Several GRB properties are affected by the jet structure: the achromatic break $t_{\rm break}$ in the afterglow light curve is smoother in the SJ model and it is related to $\theta_{\rm v}$ rather than $\theta_{\rm j}$ (Zhang & Meszaros 2002); different degree of polarization of the afterglow emission (Rossi et al. 2004; Lazzati et al. 2004) and different luminosity functions (and GRB rates) are expected in the two scenarios. The jet break measurements are hampered by the necessity of a follow up of the afterglow emission until late times, by the smoothing induced by viewing angle effects (e.g. van Eerten & MacFadyen 2012) and by the contamination of the afterglow emission at late times by the possible supernova and host galaxy emission (e.g. Ghirlanda et al. 2007). Despite all these diagnostics, there is no concluding evidence yet of the real jet structure. On the other hand, the increasing number of bursts with measured redshift allows to estimate the luminosity function of GRBs with increasing confidence. We show in this paper how the jet structure affects the observed luminosity function.

The most recent studies of the GRB luminosity function are by Wanderman & Piran 2010 with a relatively large GRB sample, and by Salvaterra et al. (2012) with a relatively small but complete GRB sample. GRBs with measured redshift have typical isotropic equivalent luminosities in the range 10^{50-54} erg s^{-1}. At lower luminosities the detection rate drops to only a few events which are, however, representative of a large local density of GRBs (e.g. Soderberg et al. 2006; Pian et al. 2006). Indeed, it has been suggested that these latter events could belong to a different GRB population (e.g. Virgili et al. 2009; Daigne & Mochkovitch 2007).

1.1 Structure of this work

In this paper we first consider the low luminosity GRBs to discuss if they can be accounted for by the extrapolation of the luminosity function (LF) describing high luminosity GRBs (§2). In this case we would have a luminosity function (LF) extending over 7 orders of magnitude to be compared with different models. Then we study four different possibilities:

(i) First we consider the simplest model: all jets are uniform, with the same $\theta_{\rm j}$ and are seen always on–axis, but we assume that the jet had to punch the progenitor star before emerging, and in so doing it must spend $\sim 10^{51}$ erg. We derive the predicted LF in this case, and compare it to the data (§3.1.1).

(ii) Then we allow $\theta_{\rm j}$ to vary as a function of the observed luminosity, but we still assume that all bursts are seen on–axis. Bursts of equal collimation corrected luminosity, but of different $\theta_{\rm j}$ will have different isotropically equivalent luminosities $L_{\rm iso}$ (the smaller $\theta_{\rm j}$, the larger $L_{\rm iso}$). Also in this case we can construct analytically the LF, and we compare it with the data (§3.1.2)

(iii) We consider the possibility that (some) GRBs can be detected even if observed off–axis, even if the jet is uniform. In fact any GRB will emit not only within $\theta_{\rm j}$, but also outside, even if the corresponding radiation is not as relativistically boosted as the radiation inside the jet cone. The observable off–axis luminosity depends on the bulk Lorentz factor (the larger Γ, the dimmest the off–axis luminosity). The predicted LF for a single value of Γ and $\theta_{\rm j}$ can be derived analytically, allowing for an easy numerical computation of the LF with a distribution of Γ and $\theta_{\rm j}$. The latter is compared to the data (§3.2).

(iv) Finally, we consider structured jets, characterized by a power law dependence of the radiated energy with the angle from the jet axis ($E \propto \theta^{-s}$) to find out if the data are consistent with this scenario, and for which slope s (§4).

We discuss our results in §5. In the paper we assume a standard flat cosmology with $h = \Omega_\Lambda = 0.7$.

2 LONG GRB LUMINOSITY FUNCTION

The problem of deriving the luminosity function [LF – $\Phi(L)$] of GRBs has been approached by different authors (Firmani et al. 2004; Guetta et al. 2005; Natarajan et al. 2005, Daigne et al. 2006, Salvaterra & Chincarini 2007; Salvaterra et al. 2009; 2012) by convolving $\Phi(L)$ with the GRB formation rate $R_{GRB}(z)$ (proportional to the cosmic star formation rate). The free parameters of the LF can be constrained by fitting the resulting model to the flux distribution of large GRB samples (e.g. the *CGRO*/Batse population). Note that, in the GRB literature, it is customary to consider as cosmic evolution any (i.e. density, or luminosity, or both) evolution *in addition* to the one related to the evolution of the star formation rate. The main difficulty of these studies is accounting, in the model, for the selection effects which affect the true GRB population detected by any instrument. Recently, Salvaterra et al. (2012 – S12 hereafter) constructed a flux limited sample of bright GRBs detected by *Swift*/BAT which resulted 95% complete in redshift. While the possible evolution of the luminosity function or of the GRB formation rate with redshift is still a matter of debate, there seems to be a general consensus on the shape of the LF:

$$\Phi(L) \propto \begin{cases} \left(\frac{L}{L_{\rm c}}\right)^{-a}, & L \leqslant L_{\rm c} \\ \left(\frac{L}{L_{\rm c}}\right)^{-b}, & L > L_{\rm c} \end{cases} \quad (1)$$

where L_c represents the break luminosity. S12 finds $a = 1.56^{+0.11}_{-0.42}$, $b = 2.31^{+0.35}_{-0.31}$, $L_c = 2.5^{+6.8}_{-2.1} \times 10^{52}$ erg s^{-1} (68% confidence intervals) for the case of no evolution of $\Phi(L)$.

2.1 High Luminosity (HL) GRBs

Wanderman & Piran (2010) (WP10 hereafter) adopted a direct inversion method on the distribution of GRBs in the $L - z$ space obtaining simultaneously $\Phi(L)$ and R_{GRB} independently[1]. They

[1] This method relies on the assumption of no evolution of the GRB luminosity function and rate with redshifts. See WP10 for the validity of this assumption.

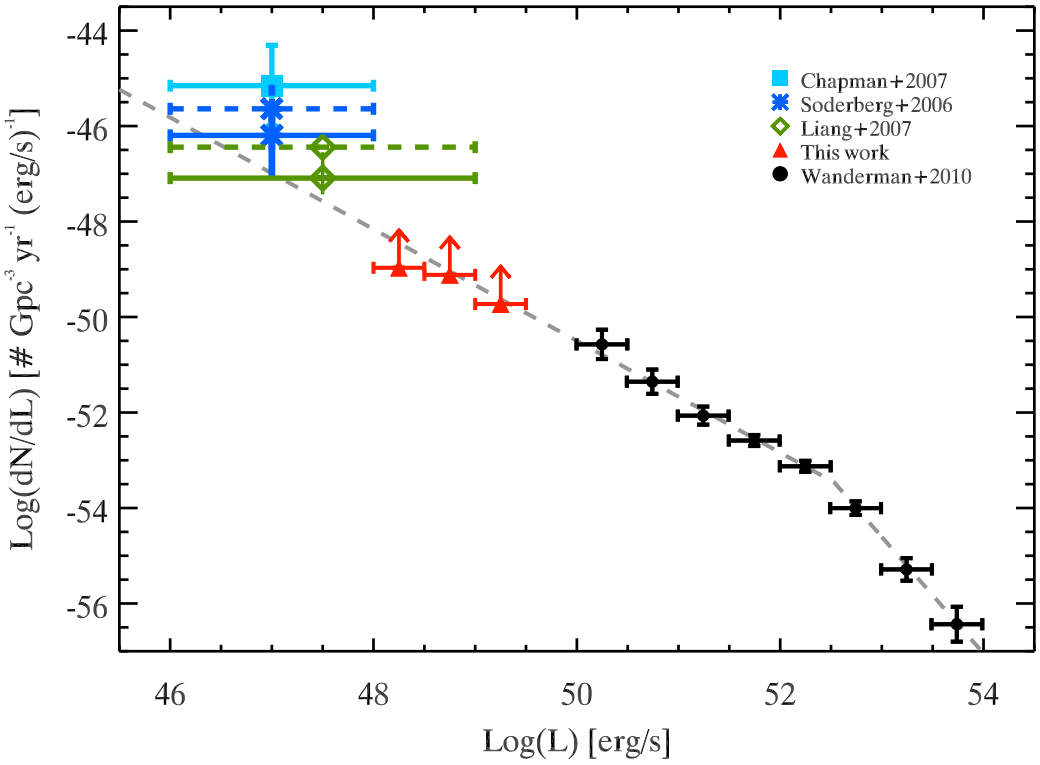

Figure 1. Long GRB luminosity function representing the number of GRBs per unit volume, time and luminosity bin. Black symbols represent the discrete luminosity function of WP10. The grey dashed line is the empirical fit of WP10 with a broken power law with $a = 1.2$, $b = 2.4$ and $L_{\rm c} = 3.2 \times 10^{52}$ erg s^{-1}. The rate of low luminosity GRBs is shown with different symbols according to the different sources in the literature: asterisk (Soderberg et al. 2006), diamond (Liang et al. 2007), filled square (Chapman et al. 2007). The Soderberg et al. (2006) and Liang et al. (2007) rates were calculated assuming a time bin corresponding to the *Swift* lifetime in 2006 (points with dashed horizontal bars). Since then, no other burst in the same luminosity bin has been discovered, so we added the rates corrected for the current *Swift* lifetime (points shown with solid horizontal bars). The lower limits on the rate of intermediate luminosity GRBs (IL) added in this work are shown with the filled (red) triangles.

selected a sample of long[2] GRBs with spectroscopically measured redshift and isotropic equivalent luminosities $L_{\rm iso} \geqslant 10^{50}$ erg s^{-1} detected by BAT on board *Swift*. The derived LF is represented by a discrete series of data points (Fig. 3 of WP10) in eight equal logarithmic bins of luminosity and can be represented by a broken power law with $a = 1.2^{+0.2}_{-0.1}$ and $b = 2.4^{+0.3}_{-0.6}$, with the break at $L_{\rm c} = 10^{52.5\pm0.2}$ erg s^{-1} (note that WP10 use $dN/d\log L$, whereas we prefer to adopt $dN/dL = dN/(L\, d\log L)$ so that the WP10 slopes are here increased by 1).

These parameter values are consistent with those derived with the "classical" approach described above. We normalized the luminosity function at the local GRB rate $\rho_0 \simeq 1.3$ Gpc^{-3} yr^{-1} (WP10). Fig. 1 shows the data points of WP10 (black symbols) which cover the luminosity range between 10^{50} and 10^{54} erg s^{-1} and will be referred to as HL bursts hereafter. The best fit obtained by WP10 is shown as a grey long dashed line.

2.2 Low Luminosity (LL) GRBs

At the low end of the luminosity distribution of GRBs, i.e. $L_{\rm iso} \sim 10^{46-48}$ erg s^{-1}, there are two events (GRB 980425 and GRB 060218) which have been detected in the local Universe and have been intensively studied as direct evidences of the massive star progenitor of long GRBs. Their luminosity is three orders of magnitude smaller than HL bursts, and their rate is larger (e.g. Soderberg et al. 2006). GRB 980425 ($z = 0.008$, associated to SN1998bw – Galama et al. 1998) was detected by *CGRO*/Batse and had $L_{\rm iso} \sim 7 \times 10^{46}$ erg s^{-1} (as computed from its prompt emission spectrum – Jimenez, Band & Piran 2001). Similarly, GRB 060218 ($z = 0.0331$, associated to SN2006aj – Sollerman et al. 2006), detected by *Swift*/BAT, had $L_{\rm iso} \sim 1.3 \times 10^{47}$ erg s^{-1} (Campana et al. 2006) .

The rate of these LL events can be computed as

$$\rho_{LL} \simeq 4\pi \frac{N_{\rm LL}}{V_{\rm max} T \Omega} \qquad (2)$$

where $V_{\rm max}$ is the maximum volume within which they could be detected by an instrument with an assigned sensitivity, with a field of view Ω and operating for a time T. Based on the two GRBs 980425 and 060218, Soderberg et al. (2006; see also Pian et al. 2006) derived the rate of LL events by conservatively averaging over $V_{\rm max}$ and Ω for different detectors (*Beppo*SAX/WFC, *Hete–II*/WXM and *Swift*/BAT). They obtained a rate $\rho_{\rm LL} \sim 230^{+490}_{-190}$ Gpc^{-3} yr^{-1}. In the luminosity range 10^{46}–10^{48} erg s^{-1} occupied by these two GRBs and centered at $\langle L \rangle = 10^{47}$ erg s^{-1} we convert this rate dividing it for the interval width obtaining

[2] See Wanderman & Piran (2014) for the same method applied to short GRBs.

$\tilde{\rho}_{\rm LL} \sim 2.3 \times 10^{-46}$ Gpc^{-3} yr^{-1} erg^{-1} s. This is represented by the (blue) asterisk in Fig. 1. Since $\rho_{\rm LL}$ has been computed in 2006, we have also corrected it (blue asterisk with solid horizontal bar in Fig. 1) for the larger time interval elapsed since the detection of these two LL events. These results are consistent with numerical studies: Virgili, Liang & Zhang (2009) estimate ρ_{LL}=200 Gpc^{-3} yr^{-1} for events with $\langle L \rangle = 10^{47}$ erg s^{-1} based on the Batse GRB population. A slightly larger rate $\rho_{\rm LL} \sim$700$\pm$360 Gpc^{-3} yr^{-1} (shown by the cyan filled square symbol in Fig. 1) has been obtained by Chapman et al. (2007) from the cross–correlation of a subsample of low–fluence smooth single–peaked Batse bursts with nearby galaxies. Liang et al. (2007) also derived $\rho_{\rm LL} = 325^{+352}_{-177}$ Gpc^{-3} yr^{-1} (shown by the green diamond symbol in Fig. 1 and also corrected for the lifetime of *Swift*).

2.3 Intermediate Luminosity (IL) GRBs

In the intermediate luminosity range between HL and LL (see Fig. 1) we can add some constraints. We have searched all GRBs with measured redshift[3] z and with $L_{\rm iso} \in [10^{48}, 10^{50}]$ erg s^{-1}. In addition to z, we also required that $L_{\rm iso}$ is well determined: this is possible when the spectrum at the peak of the light curve has been fitted over a wide enough energy range as to constrain its peak energy. Indeed, in these cases it is possible to compute the bolometric isotropic luminosity. We adopted the same method described for LL (from Soderberg et al. 2006) to compute $\rho_{\rm IL}$ in three luminosity bins, using the following bursts: (i) GRB 051109B with $L_{\rm iso} \in [10^{48}, 3 \times 10^{48}$ erg s$^{-1}]$, (ii) GRB 020903, 031203, 060505 with $L_{\rm iso} \in [3 \times 10^{48}, 10^{49}$ erg s$^{-1}]$ and (iii) GRB 120422A, 130702 with $L_{\rm iso} \in [10^{49}, 3 \times 10^{49}$ erg s$^{-1}]$.

We have collected the prompt emission spectral parameters and flux of these bursts (reported in Tab. 1 – Col. 4–8) through which we have computed their bolometric flux (Col. 11 in Tab. 1). Three different instruments were involved in triggering these events (Col. 10 in Tab. 1) and we considered the following instrumental parameters: $\Omega = 1.33$ sr and $T = 8$ yr for *Swift*, $\Omega = 0.1$ sr and $T = 10$ yr for *Integral* and $\Omega = 0.802$ sr and $T = 4$ yr for *Hete–II*. The last column in Tab. 1 reports the limiting flux of the corresponding detectors as computed by Band (2002; 2006) which depends on the burst peak spectral energy $E_{\rm peak}$ (in the observer frame). $P_{\rm lim}$ as computed by Band (2002; 2006) in the [1-1000] keV observed energy band is used to compute the maximum distance (and therefore $V_{\rm max}$) out to which these events could have been detected. With the same method adopted for LL bursts we could derive a rate ρ_{IL} for intermediate luminosity events. These rates should be considered as lower limits: we only selected GRBs with measured redshifts and well constrained spectral parameters. These are most likely only a fraction of the bursts, with similar luminosities, which effectively triggered the corresponding detector. These rates are shown by the (red) triangles in Fig. 1.

Finally, Fig. 1 shows the luminosity function of HL bursts (data points from WP10 – black symbols), IL bursts (lower limits – red triangles) and LL bursts (colored symbols - references in the caption). The grey dashed line represents the LF fitted by WP10 to their data points (only HL bursts) and it can be noted that its extrapolation to low luminosities is consistent with both the lower limits of IL bursts and the rate of LL events. This is a direct indication that LL and HL have a common progenitor, i.e. they form a *unique population*. Apparently there is no need to invoke a different origin for the LL events as they are consistent with the extension to low luminosities of the LF of HL bursts. Based on this evidence, in the following we compare the empirical LF with model predictions for different jet configurations.

[3] http://www.mpe.mpg.de/∼jcg/grbgen.html

3 UNIFORM JET

In this section, we derive the analytic expression of the luminosity function under the assumptions of UJ, e.g. we assume that the energy per unit solid angle ϵ and the initial bulk Lorentz factor Γ_0 are constant within the jet, and zero outside.

3.1 Jet break–out energy

To be observed, the jet must emerge from the progenitor star. This implies that a minimum central engine duration is required for a jet to successfully escape the progenitor star. Bromberg et al. (2012) derived interesting consequences from this simple consideration, concerning the GRB duration distribution. If the central engine lasts much longer than the time necessary for the jet to drill through the star (break out time), the resulting GRB will be a long one. If the central engine duration is comparable to the break out time, but slightly longer, the GRB will be short. As a consequence Bromberg et al. (2012, 2013) estimated the fraction of short GRBs produced by collapsars and revised the separation of long/short events.

The same argument can be applied to the energetics. In a recent work Kumar & Smoot (2014) find that the minimum energy required to excavate the star envelope must be at least the energy contained in the cocoon. Based on Mészáros & Rees (2001) we assume that the energy associated to the cocoon is $E_\star \simeq 10^{51}$ erg.

Therefore, if the inner engine provides enough energy $E_{\rm kin} > E_\star$, the jet can escape the star and the GRB can be observed. The "residual" energy of the burst will be $E_{\rm kin} - E_\star$. If $E_{\rm kin} \gg E_\star$, a normal HL burst is observed, while LL events are those with $E_{\rm kin}$ only slightly larger than $E_\star$. We show below that, likewise to the duration distribution (Bromberg et al. 2012), also the energy distribution should be flat below the characteristic $E_\star$.

Assume that the central engines of GRBs provide a total kinetic energy distributed as $P(E_{\rm kin}) = dN(E_{\rm kin})/dE_{\rm kin} \propto E_{\rm kin}^{-k}$. Of the total kinetic energy $E_{\rm kin}$ produced by the central engine, only $E_{\rm kin} - E_\star$ is available, left after the jet has escaped the progenitor star. Moreover, only *a fraction* η of the residual kinetic energy $E_{\rm kin} - E_\star$ can be converted into radiation (η is typically a few per cent in the standard internal shock model – Rees & Meszaros 1994).

If $E_\gamma = \eta(E_{\rm kin} - E_\star)$ is the energy converted into radiation, we can define its isotropic equivalent as:

$$E_{\rm iso} = \frac{\eta(E_{\rm kin} - E_*)}{1 - \cos\theta_{\rm j}} \tag{3}$$

where $\theta_{\rm j}$ is the jet opening angle. The relation between $P(E_{\rm kin})$ and $P(E_{\rm iso})$ is:

$$P(E_{\rm iso}) = P(E_{\rm kin}) \frac{dE_{\rm kin}}{dE_{\rm iso}} \tag{4}$$

To pass from the energy function to the luminosity function we take advantage of the fact that the distribution of the rest frame duration of GRBs peaks at 25 s. This is true also for the bursts used by WP10. Assuming that the light curve of the prompt emission can be approximated by a triangular shape, we have $E_{\rm iso} \approx (t \times L_{\rm iso})/2$.

GRB	z	Ref[a]	α	β	$E_{\rm peak}$ keV	P ph/cm^2/s	ΔE keV	Ref[b]	$P_{\rm bol}$ ph/cm^2/s	$L_{\rm iso}$ erg/s	Instr.	$P_{\rm lim,bol}$ ph/cm^2/s
020903	0.25	1	–1.0	...	3.37	2.8	[2–400]	7	6.52	4.86×10^{48}	*Hete–II*	3.0
031203	0.105	2	–1.63	...	144	2.2	[15–150]	8,9,10	17.9	10^{49}	*Integral*	3.0
051109B	0.08	3	–1.90	...	50†	0.5	[15–150]	11,12,13	9.43	1.64×10^{48}	*Swift*	1.3
060505	0.089	4	–1.8	...	239†	1.9	[15–150]	11	8.0	7.14×10^{48}	*Swift*	0.8
120422A	0.283	5	–1.94	...	53	0.6	[15–150]	14	11.35	2.7×10^{49}	*Swift*	2.5
130702A	0.145	6	–1.0	–2.5	20	7.03	[10–1000]	15	7.03	2.87×10^{49}	*Swift*	2.5

Table 1. Intermediate Luminosity (IL) GRBs. [a] References for the redshift: (1) GCN #1554 Soderberg, Price, Fox et al. (2002); (2) GCN #2482 Prochaska, Bloom, Chen, Hurley, Dressler & Osip (2003); (3) GCN # 5387 Perley, Foley, Bloom & Butler (2005) ; (4) GCN #5161 Thoene, Fynbo, Sollerman et al. (2006); (5) GCN #13251 Tanvir, Levan, Cucchiara et al. 2012 ; (6) GCN #14983 Leloudas, Fynbo, Schulze et al. (2013); [b] References for the spectral parameters: (7) Sakamoto et al. (2004) ; (8) Bosnjak et al. (2013); (9) Sazonov et al. (2004); (10) Ulanov et al. (2005); (11) Troja et al. (2006); (12) Sakamoto et al. (2009); (13) Butler et al. (2007); (14) Zhang et al. (2012); (15) Kienlin et al. (2014). † $E_{\rm peak}$ computed through the $\alpha - E_{\rm peak}$ correlation of Sakamato et al. (2009) for *Swift* GRBs (for GRB 051109B consistent also with the estimate of Butler et al. 2007).

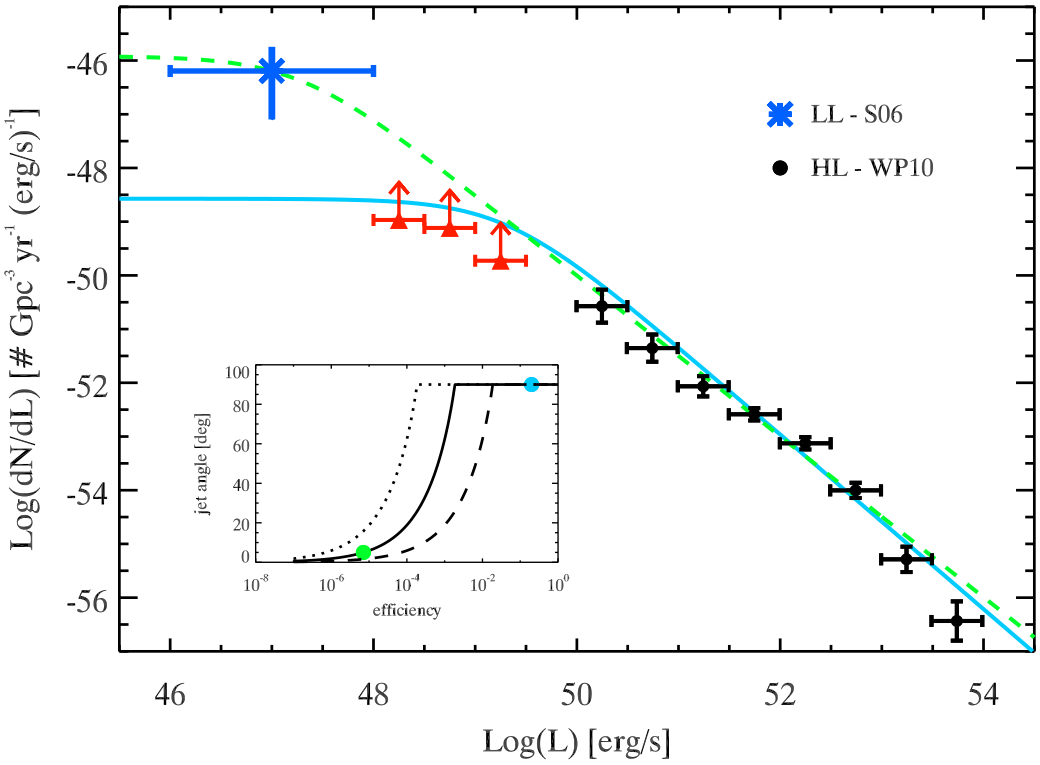

Figure 2. Luminosity function fitted with the UJ model (Eq. 6) with fixed opening angle. For the models shown in the main plot (solid cyan and dashed green curves) $L_\star = 10^{50}$ erg s^{-1} is fixed. The solid cyan line shows the case with $\eta = 0.2$ (which gives $\theta_{\rm j}$=90°) and the dashed green line is the case with $\theta_{\rm j}$=5° (which gives $\eta \sim 10^{-5}$). *Inset*: curves showing the degeneracy of the model in the angle and efficiency parameters. Dotted, solid and dashed curves correspond to different choices of $L_\star = 10^{49}, 10^{50}, 10^{51}$ erg s^{-1}, respectively. The green and cyan dots show the choice of η and $\theta_{\rm j}$ corresponding to the model curves shown in the main panel, respectively.

Then the luminosity function in the UJ model is:

$$P(L_{\rm iso}) = P(L_{\rm kin})\frac{dL_{\rm kin}}{dL_{\rm iso}} = L_{\rm kin}^{-k}\frac{1-\cos\theta}{\eta} \propto \frac{(1-\cos\theta_{\rm j})}{\eta}\left[\frac{L_{\rm iso}(1-\cos\theta_{\rm j})}{\eta}+L_\star\right]^{-k} \quad (5)$$

where $L_\star$ is the collimation corrected (i.e. "true") *kinetic* luminosity necessary to punch the star, while $L_{\rm iso}$ is the observed, isotropically equivalent *radiative* luminosity. Eq. 5 is the LF of *all* bursts, including the ones not pointing at us. If all bursts have the same $\theta_{\rm j}$, we will see only a fraction $(1-\cos\theta_{\rm j})$ of them, independent of luminosity. Therefore the observed LF is:

$$P(L_{\rm iso}) \propto \frac{(1-\cos\theta_{\rm j})^2}{\eta}\left[\frac{L_{\rm iso}(1-\cos\theta_{\rm j})}{\eta}+L_\star\right]^{-k} \quad (6)$$

Only those engines providing $L > L_\star$ will produce a successful GRB and build up the $P(L_{\rm iso})$ distribution: if $L \gg L_\star$ then

$P(L_{\rm iso}) \propto L_{\rm iso}^{-k}$, whereas for $L \lesssim L_\star$ the luminosity function is flat:

$$P(L_{\rm iso}) \propto \begin{cases} {\rm const}, & L_{\rm iso} \ll \eta L_\star/(1-\cos\theta_j) \\ L_{\rm iso}^{-k}, & L_{\rm iso} \gg \eta L_\star/(1-\cos\theta_j) \end{cases} \quad (7)$$

The transition between these two regimes corresponds to a characteristic luminosity, i.e. $L_{\rm iso} \sim \eta L_\star/(1-\cos\theta_{\rm j})$.

3.2 UJ observed in–jet [$\theta_{\rm v}<\theta_{\rm j}$]

Independently from the jet structure (UJ or SJ), one important parameter affecting the observed properties of GRBs is the viewing angle $\theta_{\rm v}$, i.e. the angle between the observer line of sight and the jet axis. In the UJ model, we first assume that the emission can be seen only if the observer line of sight intercepts the jet aperture angle, i.e. $\theta_{\rm v} \leqslant \theta_{\rm j}$. This is a good approximation if the bulk Lorentz factor of the prompt phase Γ_0 is relatively large, i.e. $1/\Gamma_0 \ll \theta_{\rm j}$.

3.2.1 Unique jet opening angle $\theta_{\rm j}$

Assume that all GRBs have the same $\theta_{\rm j}$. $P(L_{\rm iso})$ in Eq. 6 represents the luminosity function of the *observed* GRBs. The *total* LF is given in Eq. 5. The factor $(1-\cos\theta_{\rm j})$ is in this case constant, and can be absorbed in the normalization of Eq. 6. Fig. 2 shows the fit of the luminosity function with the model of Eq. 6. We fit the HL rates (black symbols) and the LL rate (blue asterisk) as derived by Soderberg et al. (2006 – corrected in this work for the elapsed time, see §2). The lower limits of IL bursts (red triangles in Fig. 2) are used only for a consistency check of the fitted model.

Fixing $L_\star = 10^{50}$ erg s^{-1}, the free parameters are the normalization, the slope k and the characteristic luminosity $L_\star\eta/(1-\cos\theta_{\rm j})$. Since the model depends on the ratio between η and $(1-\cos\theta_{\rm j})$, there is degeneracy between these two quantities. The fit can constrain this ratio rather than the two factors independently. We consider two cases:

- η=0.2 (as typically found from the modeling of the GRB afterglows – e.g. Panaitescu & Kumar 2002): the fit is shown by the solid cyan line in Fig. 2. HL bursts can be reproduced with a unique LF which has a slope $k = 1.62 \pm 0.08$ (1σ confidence) and is also marginally consistent with the IL lower limits. The fit has $\chi^2 = 33.5$ for 6 degrees of freedom (dof) corresponding to a goodness of fit probability of 8×10^{-6}. However, the LL bursts cannot be reproduced by this model. Indeed, the characteristic luminosity $L_\star\eta/(1-\cos\theta_{\rm j})$, with $\eta = 0.2$ and $L_\star = 10^{50}$ erg s^{-1}, corresponds to $\sim 2\times10^{49}/(1-\cos\theta_{\rm j})$ erg s^{-1}. This expression has a minimum for $\theta_{\rm j}$=90°. In this case all GRBs would be isotropic and still LL events should be a different population;
- $\theta_{\rm j}$=5° (i.e. corresponding to the typical opening angle of GRBs – Frail et al. 2001; Ghirlanda et al. 2007): the fit is shown by the dashed green line in Fig. 2 and can reproduce all the bursts (with a $\chi^2 = 16$ for 6 dof, i.e. probability 0.01). The resulting $k = 1.49 \pm 0.08$ is consistent with the previous one, but the efficiency $\eta \sim 10^{-5}$ is unreasonably low.

We have verified that the above results are independent from the choice of the particular value for $L_\star$: if we fix this parameter to any value $[10^{49}, 10^{51}]$ erg s^{-1}, we still find an unreasonably low efficiency $\eta < 10^{-5}$ for "reasonable" $\theta_{\rm j}$; or too large $\theta_{\rm j}$ for "reasonable" efficiencies. This is shown in the inset of Fig. 2 where all the curves saturate at 90° (for the three different choices of $L_\star$) for $\eta > 0.01$.

We conclude that the UJ model (assuming a unique angle for all bursts) does not reproduce the entire LF (from LL to HL bursts).

3.2.2 Jet angle depending on luminosity [$\theta_{\rm j}(L)$]

The assumption made in the previous section, that all GRBs have the same jet angle, may be relaxed. Indeed there is the possibility that the LL bursts have wide opening angles to account for their low luminosity. If the luminosity range of the LF is due to the range of opening angles, one should expect an anti correlation between $L_{\rm iso}$ and $\theta_{\rm j}$. Indeed, it has been shown that such a relation exists for GRBs with measured $\theta_{\rm j}$ (e.g. Lloyd–Ronning et al. 2004; Firmani et al. 2005; Ghirlanda et al. 2005).

The peak energy $E_{\rm peak}$ of GRBs is correlated with the isotropic energy $E_{\rm iso}$ as $E_{\rm p} = k_A E_{\rm iso}^A$ (Amati et al. 2002) with $A \sim 0.5$ (a similar correlation exists with the isotropic luminosity: $E_{\rm p} = k_Y L_{\rm iso}^Y$ – Yonetoku et al. 2004). The slopes of these two correlations are similar $A \sim Y \sim 0.5$.

If $E_{\rm iso}$ is corrected for collimation, namely $E_\gamma = E_{\rm iso}(1-\cos\theta_j)$, a tighter and steeper correlation $E_{\rm p} = k_G E_\gamma^G$ (Ghirlanda et al. 2004) is found. The slope depends on the density profile of the circumburst medium, being $G = 0.7$ for a homogeneous density and $G = 1$ for a wind profile (Nava et al. 2006). Since the $E_{\rm p} - E_{\rm iso}$ and $E_{\rm p} - E_\gamma$ correlations differ for the collimation factor (i.e. $1-\cos\theta_{\rm j}$), their different slopes suggest that there is a relation between the average jet opening angle and the energy of GRBs: more energetic bursts should have a smaller $\theta_{\rm j}$.

We can derive this relation by combining the correlations:

$$1-\cos\theta_{\rm j} = \left(\frac{k_A}{k_G}\right)^{\frac{1}{G}} E_{\rm iso}^{\frac{A-G}{G}} = C L_{\rm iso}^{-\xi} \quad (8)$$

where $\xi = (G-A)/G$. The typical duration, assumed $t = 25$ s (rest frame) to convert energetics to luminosities, has been incorporated in the normalization constant C. This relation also establishes that there is a characteristic minimum luminosity $L_{\rm iso,min} \sim 7\times10^{46}$ erg s^{-1} corresponding to $\theta_{\rm j} = 90°$.

Since $\theta_{\rm j}$ is not constant, it is convenient to find the LF of all bursts, including the ones not pointing at us, i.e. using Eq. 5. The luminosity function then becomes:

$$P(L_{\rm iso}) \propto \frac{C(1-\xi)L_{\rm iso}^{-\xi}}{\eta}\left(\frac{CL_{\rm iso}^{1-\xi}}{\eta} + L_\star\right)^{-k} \quad (9)$$

where the factor $(1-\xi)$ comes from the derivative $dL_{\rm kin}/dL_{\rm iso}$ in which now also the collimation factor depends on $L_{\rm iso}$. At low $L_{\rm iso}$, $N(L_{\rm iso}) \propto L^{-\xi}$, while at large $L_{\rm iso}$, $N(L_{\rm iso}) \propto L^{-\xi-k(1-\xi)]}$. The break is at $L_{\rm iso} \sim (\eta L_\star/C)^{1/(1-\xi)}$.

In Fig. 3 the corrected points (black dots and red triangles) are shown together with the observed ones (grey dots): the higher the luminosity, the larger is the applied correction, according to Eq. 8. Below a limiting $L_{\rm iso}$ the opening angle becomes larger than 90° and we do not apply the correction any longer. Since smaller angles correspond to larger $L_{\rm iso}$, the LF of all GRBs is flatter than the observed one.

Fixing $L_\star = 10^{50}$ erg s^{-1}, the fit favors an efficiency $\eta = 1$ (pegged to its maximum value) which is unrealistic (e.g. there would be no energy left for the afterglow emission). Similarly to the previous case, changing $L_\star$ by a factor 10 still gives $\eta = 1$. This is due to the degeneracy between η and $L_\star$. Only for $L_\star \geqslant 10^{52}$ erg s^{-1} we find reasonable values of η. Therefore, we decided to show in Fig. 3 the fit with both η and $L_\star$ fixed to their typical values (0.2

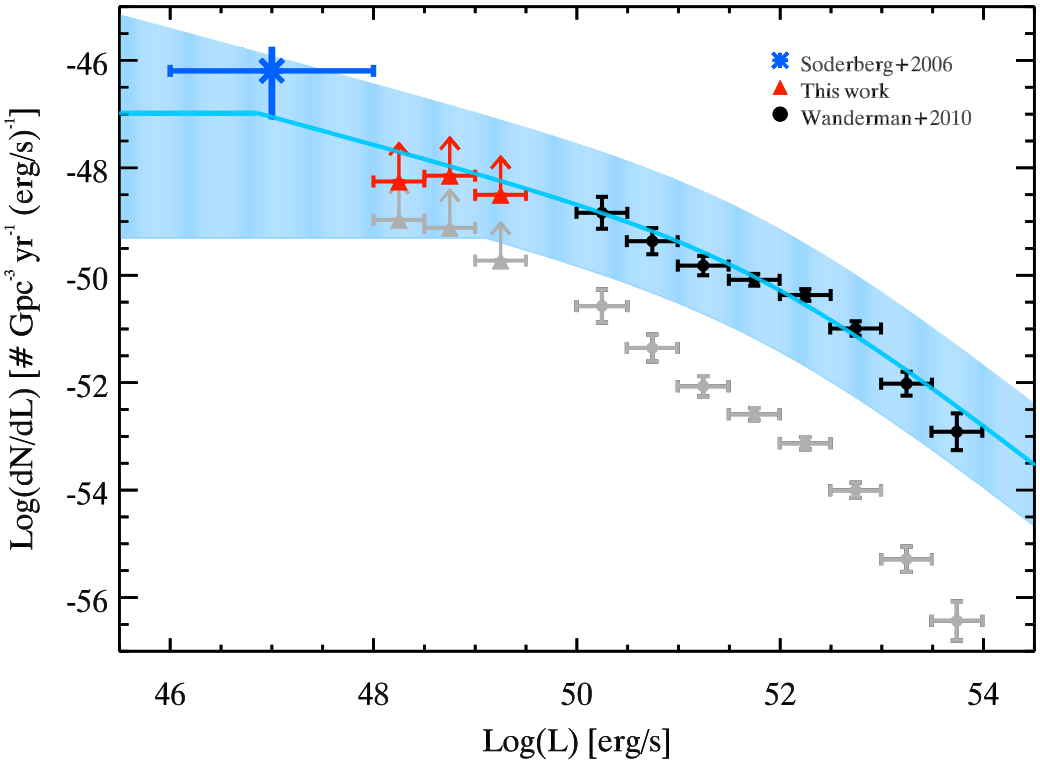

Figure 3. Uniform Jet with jet angle dependent from the luminosity. The LF of the entire GRB population (i.e. corrected for the collimation factor, which depends on the luminosity in this case) is shown by the black symbols. Original points (grey symbols) are also shown. The model is shown by the solid cyan line and the 3σ confidence interval of the model, obtained accounting for the scatter of the $\theta_{\rm j}$–$L_{\rm iso}$ correlation (see text) is shown by the azure shaded region.

and 10^{50} erg s^{-1} respectively) (cyan solid line). The fit is consistent with the lower limits of the IL bursts (triangles in Fig. 3) and marginally consistent with the LL bursts. Setting $A = 0.5$, $G = 1$, we have $\xi = 0.5$, which is the slope at low luminosities. The slope of the distribution of energies provided by the inner engine found by the fit is $k = 1.5 \pm 0.15$, corresponding to an high luminosities slope $\xi + k(1-\xi) \simeq 1.25$ for $\Phi(L)$. We stress that "finding the best fit" is here only a formal procedure: to the errors associated with the data points we should in fact add the uncertainties about the $E_{\rm p} - E_{\rm iso}$ and $E_{\rm p} - E_{\gamma}$ correlations, that have a scatter of 0.22 dex and 0.12 dex, respectively. Fig. 3 shows (shaded region) the 3σ boundaries of the LF obtained accounting for the scatter of these correlations in deriving the correlation of Eq. 8. The LL point is at the border of this confidence interval.

3.3 UJ observed in– and out–jet [$\theta_{\rm v} \lessgtr \theta_{\rm j}$]

In the previous subsections we assumed that we can see the prompt emission of GRBs only if we are within the jet opening angle, $\theta_{\rm v} \leqslant \theta_{\rm j}$, i.e. that off–axis observers see no emission. This implies large bulk Lorenz factors, i.e. $\Gamma \gg 1/\theta_{\rm j}$. However, the slope of the LF found by WP10 below the break (dashed line in Fig. 1) is $\sim$1.25. This slope can be predicted in the case of UJ observed off–axis. To see this, consider a population of bursts $N(L_{\rm iso,on})$ that have the same $L_{\rm iso,on}$ when observed on axis. The number of bursts seen at different viewing angles will depend on the corresponding solid angle, and they will be observed with a reduced (de–beamed) luminosity L (see Ghisellini et al 2006 for GRBs; Urry & Shafer 1984 and Celotti et al. 1993 for blazars):

$$N(L, L_{\rm iso,on})dL = \frac{d\Omega}{2\pi} \rightarrow N(L, L_{\rm iso,on}) = \left(\frac{dL}{d\cos\theta}\right)^{-1} \quad (10)$$

The observed luminosity is the sum of the contributions of different portions of the emitting surface, each observed under a different angle (Ghisellini et al. 2006):

$$L(\theta_{\rm v}) = \int_{\max(0,\theta_{\rm v}-\theta_{\rm j})}^{\theta_{\rm v}+\theta_{\rm j}} \Delta\phi\, \delta^4\, L'\, \sin\theta\, d\theta \quad (11)$$

where L' is the comoving luminosity per unit solid angle (which is assumed constant throughout the entire jet surface), θ is defined as the angle between the line of sight and each emitting element of the jet and $\Delta\phi$ takes into account the geometry of the emitting surface. If the line of sight coincides with the jet axis the emitting surface is a circular corona so that $\Delta\phi = 2\pi$, while for off–axis observers this is a portion of circular corona which depends on $\theta_{\rm v}$ (Ghisellini & Lazzati 1999):

$$\Delta\phi = \begin{cases} 2\pi & \text{if } \theta < \theta_{\rm j} - \theta_{\rm v} \\ \pi + 2\sin\left(\frac{\theta_{\rm j}^2 - \theta_{\rm v}^2 - \theta^2}{2\theta_{\rm v}\,\theta}\right) & \text{if } \theta \geqslant \theta_{\rm j} - \theta_{\rm v} \end{cases} \quad (12)$$

The right panel of Fig. 4 shows the LF for different choices of $\theta_{\rm j}$ and Γ. According to the different scaling of L with $\theta_{\rm v}$ we have different slopes of the LF, which can be easily explained:

Small angles: $\theta_{\rm v} < \theta_{\rm j}$ — the observed luminosity increases only slightly by decreasing $\theta_{\rm v}$. This describes the high luminosity end of

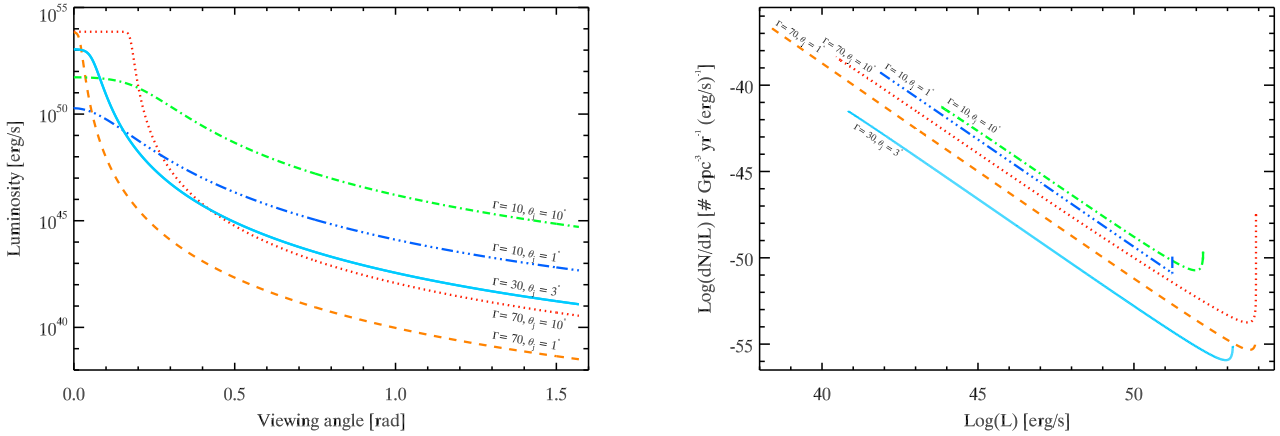

Figure 4. *Left panel*: luminosity as a function of the viewing angle for different combinations of the bulk Lorentz factor Γ and jet opening angle $\theta_{\rm j}$. The comoving frame luminosity L' is the same for all curves. The different lines (colors) show different assumed combinations of $\theta_{\rm j}$ and Γ. For all the curves we have assumed $L' = 10^{49}$ erg s^{-1}. *Right panel*: Luminosity functions corresponding to the different assumptions of $\theta_{\rm j}$ and Γ of the right panel.

the LF, in which $N(L)$ corresponds to the GRBs observable within $\theta_{\rm jet}$ (see the right panel of Fig. 4).

Intermediate angles: $\theta_{\rm j} < \theta_{\rm v} \lesssim 2\theta_{\rm j}$ — Eq. 11 shows that the luminosity depends on the bulk Lorentz factor Γ, on the jet aperture angle $\theta_{\rm j}$, and L'. Assuming $L' = 10^{49}$ erg s^{-1}, Fig. 4 (left panel) shows how $L(\theta_{\rm v})$ depends on the different choices of $\theta_{\rm j}$ and Γ. For large Γ the observed luminosity drops by a large factor when $\theta_{\rm v}$ becomes slightly larger than $\theta_{\rm j}$. This drop is smoother for smaller Γ. For $\theta_{\rm j} < \theta_{\rm v} \lesssim 2\theta_{\rm j}$ (namely, within the "jump", and before reaching the regime $L \propto \delta^4$), we can approximate the scaling of the luminosity as $L \propto \theta_{\rm v}^{-f}$. According to Eq. 10, we have:

$$N(L) \propto \left[\frac{dL}{\sin\theta d\theta}\right]^{-1} \propto \theta^{(f+2)} \propto L^{-(1+2/f)}, \quad \theta_{\rm j} < \theta \lesssim 2\theta_{\rm j} \qquad (13)$$

Note that the slope $1 + 2/f$ tends to unity for large f.

Large angles: $\theta_{\rm v} \gg \theta_{\rm j}$ — When $\theta_{\rm v} \gg \theta_{\rm j}$, the burst can be considered to have a mono–directional velocity, along the jet axis. In this case the observed luminosity is proportional to δ^4, where $\delta \equiv [\Gamma(1 - \beta\cos\theta_{\rm v})]^{-1}$ is the relativistic Doppler factor. Therefore $(dL/d\cos\theta)^{-1} \propto \delta^{-5} \propto L^{-5/4}$ [this results is general, as demonstrated by Urry & Shaefer (1984): for beaming amplification factors $L \propto \delta^p$, the resulting low luminosity branch of the observed luminosity function $N(L) \propto L^{-(1+1/p)}$].

As a first approximation consider unique values of Γ and $\theta_{\rm j}$ for all GRBs. The shapes of the corresponding LF are shown in Fig. 4 for different combinations of these two parameters, assuming a value of $L' = 10^{49}$ erg s^{-1}. The LF is a power–law with a slope $-5/4$ which smoothly turns into a peak at high luminosities corresponding to the maximum observable luminosity. The LF of GRBs shown in Fig.1 is consistent with a power–law of slope -1.2 (WP10) and breaks into a steeper (-2.4) power–law for $L_{\rm iso} > 10^{52.5}$ erg s^{-1}. Therefore, there is a very good agreement between the theoretical LF slope (Fig. 4) and the observed one below $10^{52.5}$ erg s^{-1} (Fig.1). If we assume that the break luminosity corresponds to $L_{\rm iso,on}$, i.e. of GRBs seen within the cone of their jet (i.e. those making the peak of the LF curves in Fig.4), the true rate of GRBs can be computed as $N_{\rm tot} = N_{\rm obs}/(1-\cos\theta_{\rm j})$ (where $N_{\rm obs}$ is the rate corresponding to the break of the LF of Fig. 1). Assuming that only $\sim 0.3\%$ of SNIb/c produce GRBs (e.g. Ghirlanda et al. 2013), we estimate $\theta_{\rm j} \sim 4^\circ$. The other two parameters Γ and L' of the model can be constrained requiring that the integral of the LF corresponds to $N_{\rm tot} \sim 100$ GRBs yr^{-1} Gpc^{-3}.

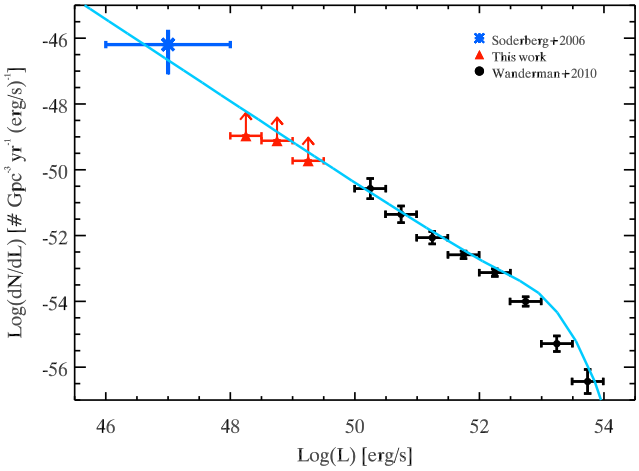

Figure 5. Uniform jet observed in and out (ref §3.3).

Still the model is not representative of the real data points, since there is the peak of the LF at the maximum luminosity (i.e. corresponding to the bursts observed within the jet aperture angle). In order to smooth this peak and obtain a break in the LF model, we introduce some dispersions of the values of Γ and $\theta_{\rm j}$. We find a good agreement with the data as shown in Fig. 5 by the solid line assuming $\theta_{\rm j}$ centered around 3° with a log–normal dispersion of width 0.2 and Γ centered at a value of 30 with a log–normal dispersion of width 0.14.

4 STRUCTURED JET

In this section we investigate the case of a structured jet (SJ), assuming that all burst have an identical structure, and that their observed properties are only due to the viewing angle $\theta_{\rm v}$. We assume

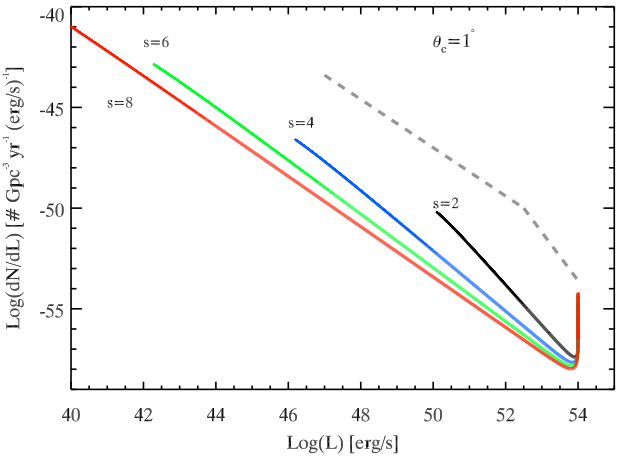

Figure 6. Structured Jet model (solid lines) for different values of the power law energy structure slope k (as labeled) assuming a core angle of 1°. The dashed grey line shows the observed luminosity function (arbitrarily rescaled for clarity) of WP10 extending from LL to HL.

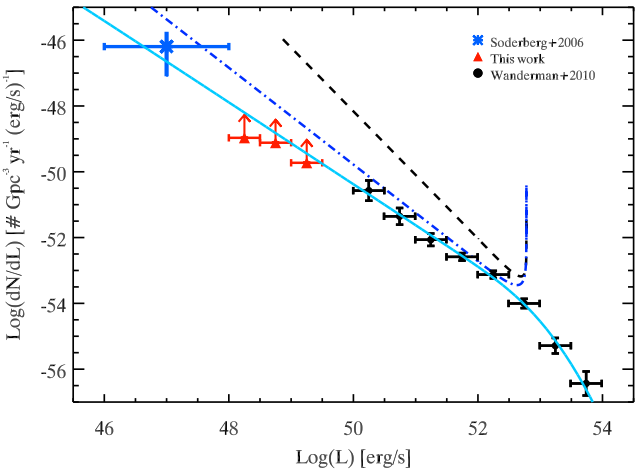

Figure 7. Structured Jet model assuming a jet core energy per unit solid angle $\epsilon_c = 6 \times 10^{52}$ erg with a dispersion (log–normal) around this value with σ=0.5, $s = 8.1$ and $\theta_c \sim 5°$. For comparison are also shown the LF obtained with $s = 2$ and $s = 4$ (from Fig.6) by the dashed and dot–dahes lines, respectively.

that the distribution of the energy per unit solid angle $\epsilon(\theta)$ is constant within a core of small aperture θ_c and distributed as a power law at larger angles:

$$\epsilon(\theta) = \begin{cases} \epsilon_c & \text{if } \theta \leqslant \theta_c \\ \epsilon_c \left(\frac{\theta}{\theta_c}\right)^{-s} & \text{if } \theta > \theta_c \end{cases} \quad (14)$$

where ϵ_c is the energy per unit solid angle within the core of the jet. The integral of $\epsilon(\theta_v)$ is the total jet energy E which is a free parameter. Different jet structures have been considered from $s = 2$ (Rossi et al. 2002) to steeper structures (Zhang & Meszaros 2002 considered also the limit of a gaussian jet). In the following s is a free parameter. We define the energy observed at a certain θ_v as $E_{\rm iso}(\theta_v) = 4\pi\eta\epsilon(\theta_v)$ and assuming a typical duration we can define the luminosity as $L_{\rm iso}(\theta_v) \propto \epsilon(\theta_v)$. For $\theta_v \leqslant \theta_c$, this corresponds to the maximum luminosity $L_{\rm iso,max} \propto \epsilon_c$. The minimum luminosity is for $\theta_v = \pi/2$. From Eq. 14 the ratio between the maximum and minimum luminosity is $L_{\rm max}/L_{\rm min} = (\pi/2\theta_c)^s$: the extension of the resulting LF is set by the slope s and the jet core θ_c. Since the observed LF of GRBs (including HL and LL bursts) extends over seven orders of magnitudes (from 10^{47} erg s^{-1} to 10^{54} erg s^{-1}), we derive the limit $s \gtrsim 7/\log[\pi/(2\theta_c)]$. A typical core angle $\theta_c = 1°$ implies $s > 3.6$, thus excluding the $s = 2$ case which is instead what required by the clustering of the collimation corrected energies of GRBs (Frail et al. 2002).

The luminosity function of the SJ results:

$$P(L_{\rm iso}) \propto \sin\left\{\left(\frac{L_{\rm iso}}{L_{\rm iso,max}}\right)^{-\frac{1}{s}}\theta_c\right\}\left(\frac{L_{\rm iso}}{L_{\rm iso,max}}\right)^{-1-\frac{1}{s}} \approx \theta_c\left(\frac{L_{\rm iso}}{L_{\rm iso,max}}\right)^{-(1+2/s)} \quad (15)$$

since the argument of the sine is always small for reasonable values of θ_c. The of the LF depends on the shape of the jet structure s which also regulates the extension of the LF (i.e. the ratio of the minimum and maximum observable luminosity) as shown by the different curves of Fig. 6. Formally, a slope $a = 1.25$ of the observed LF of Fig. 1 we get a typical value of $s = 8$. The upturn at large luminosities shown in Fig. 6 corresponds to the jets observed within the core which all have the same luminosity. Instead, the observed LF (Fig. 1) is steeper after a break corresponding to $L_{\rm iso} \sim 3 \times 10^{52}$ erg s^{-1}. To reproduce this smooth break we introduce some dispersion of the parameters. Fig. 7 shows that we can reproduce the LF if we assume a jet core energy per unit solid angle $\epsilon_c = 6 \times 10^{52}$ erg with a dispersion (log–normal) around this value with σ=0.5, $s = 8.1$ and $\theta_c \sim 5°$. The obtained LF is also consistent with the lower limits corresponding to the IL bursts.

5 DISCUSSION AND CONCLUSIONS

Due to the increased capability to measure the redshift of long GBRs, we have now better determination of their luminosity function, and indeed the results of different groups and of different methods start to converge. The LF can be modeled as a broken power law, with slopes ∼1.2–1.5 and $b > 2$, and a break above 10^{52} erg s^{-1}. The degree of cosmic evolution is instead still uncertain (see e.g. S12). Another controversial issue concerns low luminosity GRBs. We have observed very few of them, but their vicinity points to a very large rate. From what we find, they lie on the extrapolation of the luminosity function that describes high luminosity events. This suggests that LL and HL bursts belong to the same population. LL bursts have luminosities of $\sim 10^{47}$ erg s^{-1} and therefore extend the range of observed GRB luminosities to seven orders of magnitude. Is this very large range produced by the different intrinsic GRB power or is it instead the result of viewing the same intrinsic phenomenon under different lines of sight? We here discuss our findings, that are summarized in Tab. 2.

- If the jets of GRBs are homogeneous and have a typical opening angle, then the observed luminosity is proportional to the energetics of the bursts after it has spent part of its initial energy to punch the progenitor star. This implies that the LF must be flat at low luminosities, and this contradicts the data. Our conclusion is that we can exclude this simple case.
- We have then examined the case of a homogeneous jet, but with a jet angle that is related to the GRB energetics: smaller θ_j correspond to larger $E_{\rm iso}$ and $L_{\rm iso}$. Since low luminosity bursts

Model	Fig.	Main requirement	Good fit?	Comment
Uniform, same $\theta_{\rm j}$	2	Flat below $\eta L_\star/\theta_{\rm j}^2$	no	No reason. param. values
Uniform, $\theta_{\rm j}(L_{\rm iso})$	3	Needs $\theta_{\rm j} \propto L_{\rm iso}^{-\xi}$, $\xi = 0.5$ or 0.3	yes	Marg. consistent with LL
Uniform, on/off–axis	5	Needs distrib. of $\theta_{\rm j}$ and Γ	yes	Marg. consistent with HL
Structured	7	Needs $\epsilon \propto \theta^{-4}$ or steeper	yes	$\epsilon \propto \theta^{-2}$ excluded

Table 2. Synoptic view of our findings.

have larger $\theta_{\rm j}$ the probability that they intercept our line of sight is greater then that for high luminosity bursts: therefore the fraction of GRBs that we detect at lower luminosities is greater than at large luminosities. If the "true" LF is flat, the observed LF is instead decreasing towards larger $L_{\rm iso}$ with a slope that depends on the chosen relation between $\theta_{\rm j}$ and $L_{\rm iso}$. The latter can be inferred by the observed spectral energy correlations, that yields $\xi = 0.5$ (in the case of a circumburst wind density profile) or $\xi = 0.3$ (homogeneous circumburst density). In this case we can obtain a reasonable agreement with the data in the entire luminosity range but the very low luminosities, where the model shows a small deficit.

- In the third case the jet is still homogeneous, but it can be seen also off axis, for viewing angles $\theta \gtrsim \theta_{\rm j}$. This is possible for Γ not extreme, as illustrated in Fig. 4: the luminosity jump at $\theta_{\rm v} \gtrsim \theta_{\rm j}$ is more pronounced for larger Γ. The LF constructed with a single value of $\theta_{\rm j}$ and Γ do not fit the data, since they show an upturn at high luminosity instead of a steepening. On the other hand, assuming some dispersion of $\theta_{\rm j}$ and Γ, we can obtain a reasonable agreement. The required average values are $< \Gamma >= 30$ and $< \theta_{\rm j} >= 3^\circ$. What is remarkable is that the analytically predicted slope at intermediate luminosities is very close to what seen.
- Finally, we have investigated structured jets, of the form $\epsilon(\theta_{\rm v}) \propto \theta_{\rm v}^{-s}$ beyond a core angle $\theta_{\rm c}$. We have found that a good fit can be obtained, but only if the slope s is rather steep, $s > 4$, with a preferred value $s \sim 8$. This is much steeper than the value $s = 2$ originally proposed to explain the clustering of E_γ found by Frail et al. (2001).

These studies indicate that the jet must have a relatively sharp cut–off. Even if an abrupt one is unphysical (all the energy contained within $\theta_{\rm j}$, and zero outside), the energy must in any case decrease rapidly with the angle from the jet axis, once it it becomes greater than the core angle $\theta_{\rm c}$. The other important overall conclusion is that although the low luminosity bursts seem not to have enough energy to punch the progenitor star, they can nevertheless understood within the same framework of large luminosity GRBs, as long as they have a larger jet angle, or they are seen off–axis. In the first case we see the little energy leftover after the jet break–out, in the latter case the apparent low luminosity is due to the large viewing angle, but the real energetics of these burst in much greater.

ACKNOWLEDGMENTS

We acknowledge ASI I/004/11/0 and the 2011 PRIN-INAF grant for financial support.

REFERENCES

Amati L., Frontera F., Tavani M. et al., 2002, A&A, 390, 81
Band D.L., 2002, ApJ, 578, 806
Band D.L., 2006, ApJ, 644, 378
Berger E., Kulkarni S.R., Pooley G. et al., 2003, Nature, 426, 154
Bromberg O., Nakar E., Piran T. & Sari R., 2012, ApJ, 749, 110
Bromberg O., Nakar E., Piran T. & Sari R., 2013, ApJ, 764, 179
Campana S., Mangano V., Blustin, A.J. et al., 2006, Nature, 442, 1008
Celotti A., Maraschi L., Ghisellini G., Caccianiga A. & Maccacaro T., 1993, ApJ, 416, 118
Chapman R., Tanvir N.R., Priddey R.S. & Levan A.J., 2007, MNRAS, 382, L21
Cui X., Liang E. & Lu R., 2005, AJ, 130, 418
Daigne F. & Mochkovitch R., 2007, A&A, 465, 1
Daigne F., Rossi E.M.; Mochkovitch R., 2006, MNRAS, 372, 1034
Firmani C., Avila-Reese V., Ghisellini G. & Tutukov A.V., 2004, ApJ, 611, 1033
Firmani C., Ghisellini G., Ghirlanda G. & Avila–Reese V., 2005, MNRAS, 360, L1
Dessart L., Livne E. & Waldman R., 2010, MNRAS, 408, 827 bf CHECK
Frail D.A., Berger E., Galama T. et al., 2000, ApJ, 538, L129
Frail D.A., Waxman E. & Kulkarni S.R., 2000, ApJ, 537, 191
Frail D.A., Kulkarni S.R., Sari R. et al., 2001, ApJ, 562, L55
Frail D.A., Soderberg A.M., Kulkarni S.R., Berger E., Yost S., Fox D.W. & Harrison F.A., 2005, ApJ, 619, 994
Galama T.J., Vreeswijk P.M., van Paradijs J., 1998, Nature, 395, 670
Ghirlanda G., Ghisellini G. & Lazzati D., 2004, ApJ, 616, 331
Ghirlanda G., Ghisellini G. & Firmani C., 2005, MNRAS, 361, L10
Ghirlanda G., Nava L., Ghisellini G. & Firmani C., 2007, A&A, 466, 127
Ghisellini G., Ghirlanda G., Mereghetti S., Bosnjak Z., Tavecchio F. & Firmani C., 2006, MNRAS, 372, 1699
Ghisellini G., Celotti A., Ghirlanda G., Firmani C. & Nava L., 2007, MNRAS, 382, L72
Jimenez R., Band D. & Piran T., 2001, ApJ, 561, 171
Lazzati D., Rossi, E., Ghisellini, G. & Rees M.J., 2004, MNRAS, 347, L1
Lazzati D. & Begelman M.C., 2005, ApJ, 629, 903
Levinson A. & Eichler D., 2003, ApJ, 594, L19
Liang E., Zhang B., Virgili F. & Dai Z.G., 2007, ApJ, 662, 1111
Lipunov V.M., Postnov K.A. & Prokhorov M.E., 2001, Astron. Reports, 45, 236
Lyutikov M. & Blandford R., 2002, Conf. on Beaming and Jets in Gamma Ray Bursts, Edited by Rachid Ouyed (astro-ph/0210671)
Lloyd–Ronning N.M., Dai X. & Zhang B., 2004, ApJ, 601, 371
Morsony B.J., Lazzati D. & Begelman M.C., 2010, ApJ, 723, 267
Natarajan P., Albanna B., Hjorth J., Ramirez-Ruiz E., Tanvir N. & Wijers R., 2005, MNRAS, 364, L8
Nava L., Ghisellini G., Ghirlanda G., Tavecchio F. & Firmani C., 2006. A&A, 450, 471
Nakar E., Granot J. & Guetta D., 2004, ApJ, 606, L37
Panaitescu A. & Kumar P., 2002, ApJ, 571, 779
Peng F., Königl A. & Granot J., 2005, ApJ, 626, 966
Perna R., Sari, R. & Frail D., 2003, ApJ, 594, 379
Pian E., Mazzali P.A., Masetti N. et al., 2006, Nature, 442, 1011
Ramirez–Ruiz E., Celotti A. & Rees M.J., 2002, MNRAS, 337, 1349
Rees M.J. & Meszaros P., 2004, ApJ, 430, L93
Rhoads J.E., 1997, ApJ, 487, L1
Rossi E., Lazzati D. & Rees M.J., 2002, MNRAS, 332 ,945
Salvaterra R. & Chincarini G., 2007, ApJ, 656, L49
Salvaterra R., Guidorzi C., Campana S., Chincarini G. & Tagliaferri G.,

2009, MNRAS, 396, 299
Salvaterra R., Campana S., Vergani S.D. et al., 2012, ApJ, 749, 68 (S12)
Sari R., Piran T & Halpern J.P., 1999, ApJ, 519, L17
Sheth K., Frail D.A., White S., Das M., Bertoldi F., Walter F., Kulkarni S.R. & Berger E., 2003, ApJ, 595, L33
Shivvers I. & Berger E., 2011, ApJ, 734, 58
Soderberg A.M., Kulkarni S.R., Nakar E. et al., 2006, Nature, 442, 1014
Starling R.L.C., Wijers R.A.M.J., Hughes M.A., Tanvir N.R., Vreeswijk P.M., Rol E. & Salamanca I., 2005, MNRAS, 360, 305
Tan J.C., Matzner C.D. & McKee C.F., 2001, ApJ, 551, 946
Urry C.M. & Shafer R.A., 1984, ApJ, 280, 569
van Eerten, H.J. & MacFadyen A.I., 2012, ApJ, 751, 155
Virgili F.J.; Liang E.–W. & Zhang B., 2009, MNRAS, 392, 91
Vlahakis N., Peng F. & Königl A., 2003, ApJ, 594, L23
Wanderman D. & Piran T., 2010, MNRAS, 406, 1944 (WP10)
Wanderman D. & Piran T., 2014, subm to MNRAS (astro–ph/1405.5878)
Woosley S.E., Heger A. & Weaver T.A., 2002, Rev. of Modern Phys., 74, 1015
Yonetoku D., Murakami T., Nakamura T., Yamazaki R., Inoue A.K. & Ioka K., 2004, ApJ, 609, 935
Zhang B. & Meszaros P., 2002, ApJ, 571, 876
Zhang W., Woosley S.E. & MacFadyen A.I., 2003, ApJ, 586, 356
Zhang W., Woosley S.E. & Heger A., 2004, ApJ, 608, 365

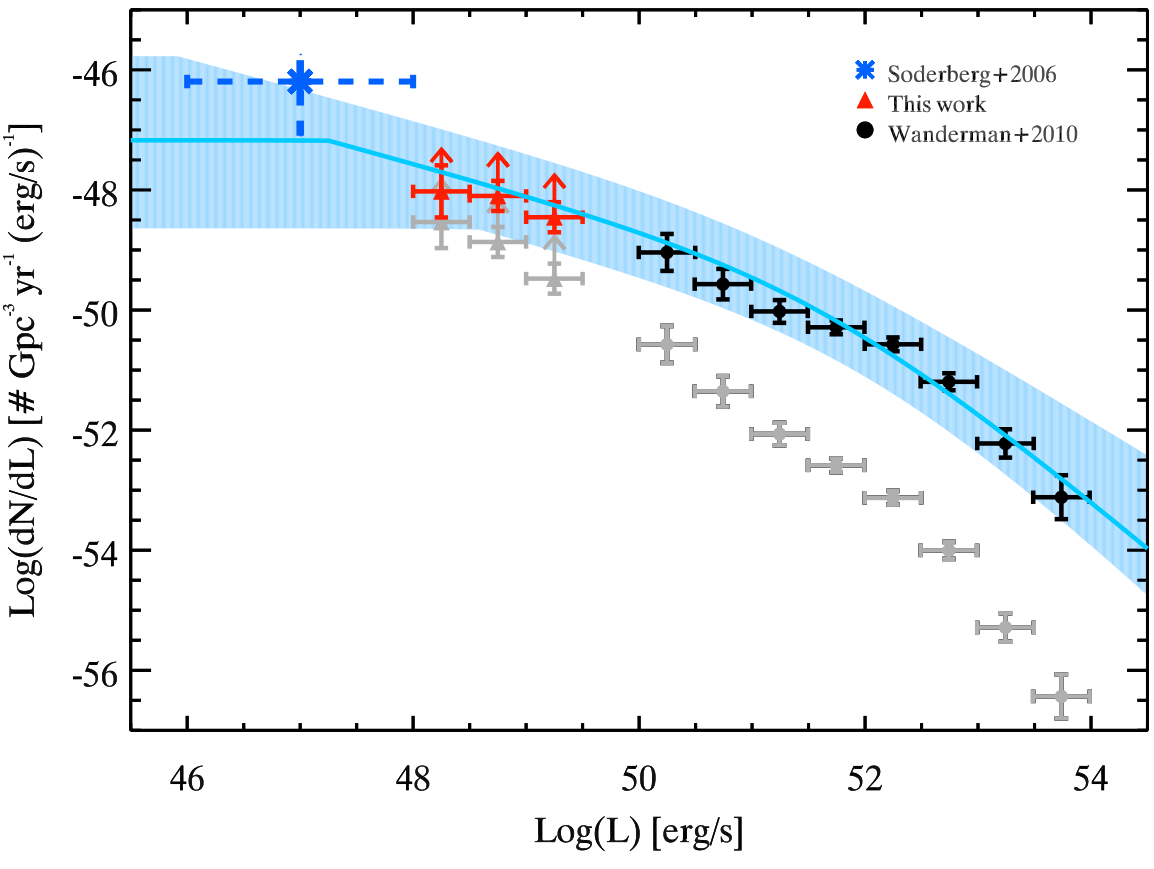
Soderberg+2006
This work
Wanderman+2010
-46
-48
-50
-52
-54
-56
46
48
50
52
54
Log(dN/dL) [# Gpc^{-3} yr^{-1} (erg/s)$^{-1}$]
Log(L) [erg/s]